2009

Timing Observations Of Rotating Radio Transients

M. A. McLaughlin

A. G. Lyne

E. F. Keane

M. Kramer

J. J. Miller

See next page for additional authors

Monthly Notices
of the
ROYAL ASTRONOMICAL SOCIETY

Mon. Not. R. Astron. Soc. **400,** 1431–1438 (2009) doi:10.1111/j.1365-2966.2009.15584.x

Timing observations of rotating radio transients

M. A. McLaughlin,[1,2★†] A. G. Lyne,[3] E. F. Keane,[3] M. Kramer,[3,4] J. J. Miller,[1] D. R. Lorimer,[1,2] R. N. Manchester,[5] F. Camilo[6] and I. H. Stairs[7]

[1]*Department of Physics, West Virginia University, Morgantown, WV 26506, USA*
[2]*National Radio Astronomy Observatory, Green Bank, WV 24944, USA*
[3]*University of Manchester, Jodrell Bank Centre for Astrophysics, Alan Turing Building, Oxford Road, Manchester M13 9PL*
[4]*Max Planck Institut für Radioastronomie, Auf dem Hügel 69, 53121 Bonn, Germany*
[5]*ATNF-CSIRO, PO Box 76, Epping, NSW 1710, Australia*
[6]*Columbia Astrophysics Laboratory, Columbia University, 550 W. 120th Street, New York, NY 10027, USA*
[7]*Department of Physics and Astronomy, University of British Columbia, 6224 Agricultural Road, Vancouver, BC V6T 1Z1, Canada*

Accepted 2009 August 19. Received 2009 August 12; in original form 2009 June 26

ABSTRACT

We present radio timing measurements of six rotating radio transient (RRAT) sources discovered in the Parkes Multibeam Pulsar Survey. These provide four new phase-connected timing solutions and two updated ones, making a total of seven of the original 11 reported RRATs now with high-precision rotational and astrometric parameters. Three of these seven RRATs have magnetic fields greater than 10^{13} G, with spin-down properties similar to those of the magnetars and X-ray detected isolated neutron stars. Another two of these RRATs have long periods and large characteristic ages, and lie near the 'death line' for radio pulsar emission. The remaining two RRATs with timing solutions have properties typical of the bulk of the pulsar population. The new solutions offer insights into what might be responsible for the unusual emission properties. We demonstrate that the RRATs have significantly longer periods and higher magnetic fields than normal radio pulsars, and find no correlation with other spin-down parameters. These solutions also provide precise positions, which will facilitate follow-up studies at high energies, crucial for relating these sources with other neutron star populations.

Key words: stars: neutron – pulsars: general – Galaxy: stellar content.

1 INTRODUCTION

In McLaughlin et al. (2006), we reported the discovery of 11 radio-emitting neutron stars characterized by repeating dispersed bursts. These 'rotating radio transients' (RRATs) have periods P ranging from 0.7 to 7 s, longer than those of most normal radio pulsars and similar to those of the populations of the X-ray detected but seemingly radio-quiet isolated neutron stars (INSs; see Kaplan 2008) and magnetars (see Woods & Thompson 2006). For the three RRATs with the highest pulse detection rates, period derivatives $\dot{P}$ were measured and reported in the discovery paper. Interpreting these $\dot{P}$ values as being due to magnetic dipole braking, they imply characteristic ages and magnetic field strengths in the general range of the normal pulsar population. One of these three RRATs, J1819−1458, however, has a magnetic field (5×10^{13} G) in the same range as the INSs and magnetars.

There have been several suggestions put forward on the nature of this new class of neutron star. The RRAT emission could be similar to that responsible for the 'giant pulses' observed from some pulsars (e.g. Knight et al. 2006). Zhang, Gil & Dyks (2007) suggest that the RRATs may be neutron stars near the radio 'death line' (Chen & Ruderman 1993) or may be related to 'nulling' (Redman & Rankin 2009) radio pulsars. Another intriguing possibility is that the sporadicity of the RRATs is due to the presence of a circumstellar asteroid belt (Li 2006; Cordes & Shannon 2008) or a radiation belt as seen in planetary magnetospheres (Luo & Melrose 2007). Alternatively, they may be transient X-ray magnetars, a relevant suggestion given the detections by Camilo et al. (2006, 2007) of transient radio pulsations from two anomalous X-ray pulsars. A final possibility is that they are similar objects to PSR B0656+14, one of three middle-aged pulsars ('The Three Musketeers'; Becker & Trümper 1997) from which pulsed high-energy emission has been detected (De Luca et al. 2005). Weltevrede et al. (2006) convincingly show that if PSR B0656+14 were more distant, its emission properties would appear similar to those of the RRATs. Radio polarization measurements of J1819−1458 also suggest properties similar to those of normal pulsars (Karastergiou et al. 2009). Determining the reason for the unusual emission of the RRATs is important since statistical analyses show that they may be up to several times more numerous in the Galaxy than the

★E-mail: maura.mclaughlin@mail.wvu.edu
†Alfred P. Sloan research fellow.

normal radio pulsars (McLaughlin et al. 2006; Keane & Kramer 2008). Furthermore, Keane & Kramer (2008) found that the Galactic supernova rate may be insufficient to account for the entire population of neutron stars. It is therefore important to know if they evolve to or from other neutron star populations, or if they are an independent and separate class. Popov, Turolla & Possenti (2006) show that the inferred birth rate of RRATs is consistent with that of INSs but not with magnetars.

To answer the above questions, phase-connected timing solutions are imperative. Periods and period derivatives allow us to compare the spin-down properties of the RRATs to those of other neutron star populations. Accurate timing positions are also crucial to facilitate high-energy observations such as the X-ray measurements of J1819−1458 which have revealed a wealth of interesting phenomenology (e.g. absorption features and extended emission cf. McLaughlin et al. 2007; Rea et al. 2009). Because of their sporadic nature, obtaining phase-connected solutions for the RRATs is a challenging endeavour and requires significant telescope resources with long observation times, along with densely spaced observing campaigns. Developing efficient methods for timing these sporadic sources is therefore crucial. This is especially important given the large number of new RRATs discovered in recent surveys [i.e. five from Deneva, Cordes & McLaughlin (2009), one from Hessels et al. (2008) and eight from Keane et al. (2009); note we do not include objects in this count which can also be detected through their time-averaged emission].

With several years of timing data obtained from the Parkes, Lovell and Arecibo telescopes, we have now been able to achieve timing solutions for four additional RRATs, bringing the total number with solutions up to seven. In addition, our continued timing observations of the three original RRATs have revealed new insights. In another paper (Lyne et al. 2009), we report the detection of glitches from J1819−1458. An updated position for J1913+1330 is reported in this paper.

In Section 2, we present the observational data. In Section 3, we describe our method for timing these sources, and present updated solutions for two RRATs and new solutions for the other four. In Section 4, we compare the spin-down properties of the RRATs with those of other neutron star populations and discuss how these new solutions impact our understanding of the nature of the RRATs. We offer conclusions and discuss plans for future work in Section 5.

2 OBSERVATIONS

The Parkes Multibeam Pulsar Survey (PMPS) covered the Galactic plane with a 13-beam 1.4-GHz receiver on the 64-m Parkes telescope in NSW, Australia. It has now discovered over 800 new pulsars (Manchester et al. 2001; Keith et al. 2009). All six of the sources discussed in this paper were discovered by McLaughlin et al. (2006) in a re-analysis of PMPS data taken between MJDs 50842 and 52324 (1998 January 29 to 2002 February 19). The sources were discovered in 35-min search observations, with between two (for J1444−6026) and six (for J1913+1330) pulses detected. Follow-up observations of the new sources with Parkes began on MJD 52863 (2003 August 15) and are on-going, with data up to MJD 54909 (2009 March 13) presented here. These observations were spaced at roughly monthly intervals, with some gaps due to telescope scheduling restrictions. All of the observations were taken using the Parkes analogue filterbanks, with 512 0.5-MHz frequency channels sampled every 100 μs with 1-bit precision. Most of the observations used the central beam of the multibeam receiver, with a central frequency of 1390 MHz and 256-MHz bandwidth. However, some observations used the 10–50 cm receiver, with a bandwidth of 64 MHz at 685 MHz (50 cm) and a bandwidth of 768 MHz at 3 GHz (10 cm) and others used the HOH receiver, which had a centre frequency of 1.5 GHz and bandwidth of 576 MHz. In addition, we have regularly observed J1913+1330 with the 76-m Lovell telescope at Jodrell Bank, using a centre frequency of 1402 MHz, and 1-bit sampled with 100-μs sampling time and 64 1-MHz channels. We have also observed this RRAT with the 305-m Arecibo telescope in Arecibo, Puerto Rico, using the Wideband Arecibo Pulsar Processor (WAPP) at a centre frequency of 327 MHz with 1024 channels spanning 25-MHz bandwidth and with three-level 128-μs sampling. The six objects for which we present timing solutions are listed in Table 1. These objects have been observed at between 49 and 71 epochs with observation lengths of 0.5–2 h for each source with Parkes. We have observed J1913+1330 with the Lovell telescope at 62 epochs with observation lengths of 1–2 h. We observed J1913+1330 with the Arecibo telescope at five epochs with observation lengths of 0.5 h each.

Note that periods for all six objects were published in McLaughlin et al. (2006). These periods were measured by calculating the differences between the arrival times of all pulses, and finding the greatest common denominator of these differences. The periods of these RRATs range from 0.77 s (J1826−1419) to 5.97 s (J0847−4316). The number of pulses detected ranges from 42 (for J1444−6026 and J1846−0257) to 348 (for J1913+1330) for the six objects presented here (Table 1). Corresponding pulse detection rates range from $0.85\,h^{-1}$ for J1444−6026 to $13\,h^{-1}$ for J1913+1330. The average peak flux densities (assuming 512 bins across the pulse period) range from 120 mJy (for J0847−4316) to 520 mJy (for J1826−1419). The maximum peak flux densities

Table 1. Timing-derived positions, distances of the timing-derived positions from the centre of the discovery-beam positions, longitudes, latitudes, DMs, distances inferred from the Cordes & Lazio (2002) model, average peak fluxes and maximum peak fluxes. The numbers in parentheses after position and DM are the 1σ errors reported by TEMPO. The distances may be uncertain by roughly 25 per cent. The peak flux densities were calculated assuming 512 bins across the pulse period. The numbers in parentheses after the average peak flux are the standard deviation.

Name	RA (J2000) ($^{h\,m\,s}$)	Dec. (J2000) ($^{\circ}\,'\,''$)	Offset (arcmin)	l ($^{\circ}$)	b ($^{\circ}$)	DM (pc cm^{-3})	Distance (kpc)	$S_{1400,avg}$ (mJy)	$S_{1400,max}$ (mJy)
J0847−4316	08:47:57.33(5)	−43:16:56.8(7)	4.4	263.4	0.16	292.5(9)	3.4	120(20)	182
J1317−5759	13:17:46.29(3)	−57:59:30.5(3)	2.3	306.4	4.7	145.3(3)	3.0	380(200)	1385
J1444−6026	14:44:06.02(7)	−60:26:09.4(4)	8.9	316.4	−0.54	367.7(1.4)	5.5	220(70)	361
J1826−1419	18:26:42.391(4)	−14:19:21.6(3)	8.0	17.4	−1.14	160(1)	3.2	520(180)	1048
J1846−0257	18:46:15.49(4)	−02:57:36.0(1.8)	2.3	29.7	−0.20	237(7)	5.2	200(60)	372
J1913+1330	19:13:17.975(8)	+13:30:32.8(1)	3.4	47.4	1.38	175.64(6)	5.7	460(260)	2040

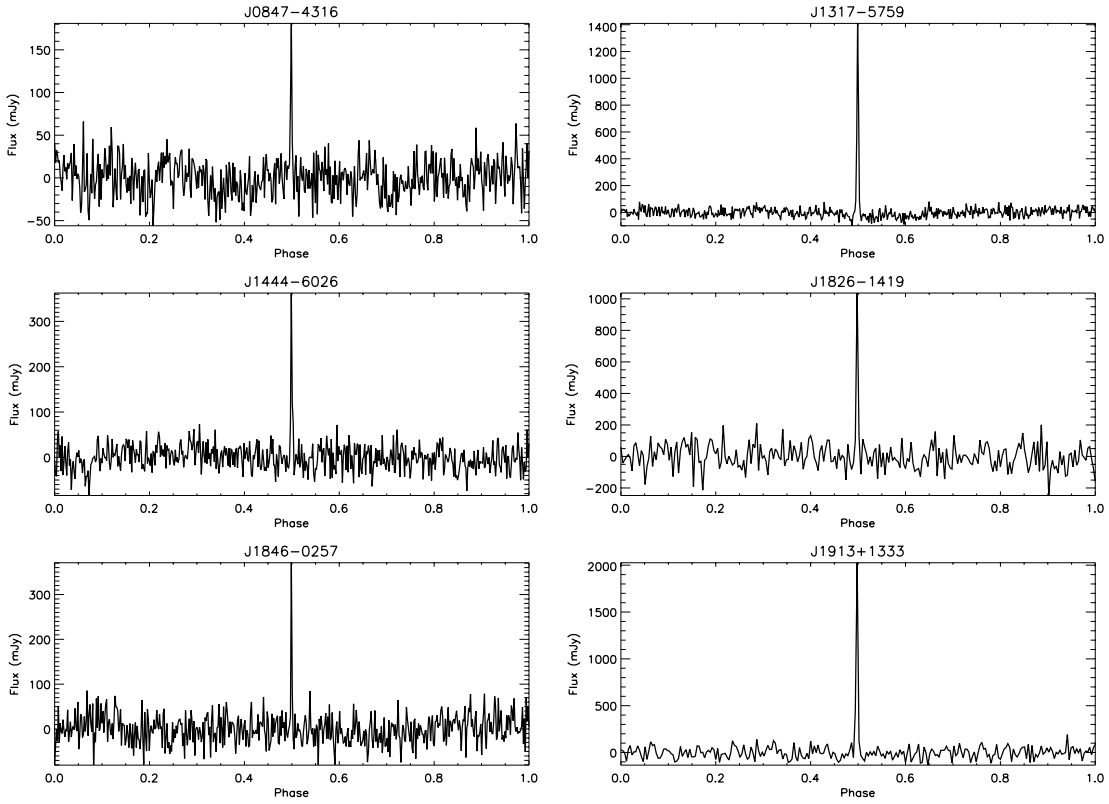

Figure 1. The brightest pulses detected in 1.4-GHz Parkes observations for all six RRATs. There are 512 bins across the pulse profile for each pulse. Flux densities have been calculated using the radiometer equation (see Lorimer & Kramer 2005), assuming a receiver temperature of 25 K and the appropriate sky temperature at 1400 MHz, scaled from the 408-MHz values of Haslam et al. (1981) assuming a spectral index of −2.6 (Lawson et al. 1987). We include a $\sqrt{2/\pi}$ loss in sensitivity for one-bit sampling.

detected for each RRAT range from 180 mJy (for J0847−4316) to 2040 mJy (for J1913+1330). In Fig. 1, we present the profiles of the brightest pulses detected from each RRAT. Inspecting the flux densities listed in Table 1 shows that the pulse amplitude distributions of the RRATs vary considerably. A detailed analysis of these distributions will be reported in a companion paper.

3 TIMING ANALYSIS AND RESULTS

In standard pulsar timing methods, pulse times-of-arrival (TOAs) are calculated through analysis of integrated profiles formed by summing many (∼thousands) of individual pulses modulo the pulse period. The sporadic nature of the RRATs' emission requires us to use single pulses instead of integrated profiles to calculate TOAs. The first step in our timing analysis is then pulse detection. This is done by dedispersing the filterbank data at the dispersion measure (DM) of the RRAT and at DM of zero, and searching for pulses in both time series above a 5σ threshold in each using the pulsar processing package SIGPROC.[1] Pulses which are brighter at the DM of the RRAT are likely to be from the source. We also inspect the pulses visually to be certain of their astrophysical nature. For some epochs which have large amounts of RFI (radio frequency interference), we applied the above procedure but with multiple trial DMs. If more than one pulse is detected within an observation, a second check based on the known period of the source can be made by requiring that all pulses have arrival times which differ by integral multiples of the period. In Table 1, we list the number of epochs for which pulses were detected for all sources. For the sources with more sporadic pulses, like J1444–6026 and J1826–1419, we detect at least one pulse in only ∼30 per cent of observations.

To calculate TOAs for normal radio pulsars, the stable integrated profiles are cross-correlated with a template profile. The single pulses of all six RRATs discussed in this paper are generally single peaked. However, the absolute phases of these peaks varies from pulse to pulse within a window that is typically a few per cent of the spin period. In addition, as for normal pulsars, the widths and shapes of the individual pulses of all six vary. In Fig. 2, we show examples of single and integrated profiles for observations of J1317−5759 and J1913+1330. Because of this intrinsic single pulse width variation, common to normal pulsars (e.g. Champion et al. 2005), fitting all single pulses to the same template results in large systematic errors. We therefore fold the single pulses with 512 bins across the pulse period to mitigate the effects of noise, and then calculate the TOA as the pulse maximum, weighted by the values in the two adjacent bins. The error on the TOA is simply taken as the width of a bin divided by the signal-to-noise ratio of the pulse (see Lorimer & Kramer 2005).

The method for fitting a timing model to our TOAs is identical to that for normal pulsars. We use the TEMPO software package[2] to fit a model incorporating spin period P, period derivative $\dot{P}$, right ascension (RA) and declination (Dec.) to our data. The results of these fits are shown in Tables 1 and 2. For J0847−4316, a

[1] http://sigproc.sourceforge.net

[2] http://www.atnf.csiro.au/research/pulsar/tempo

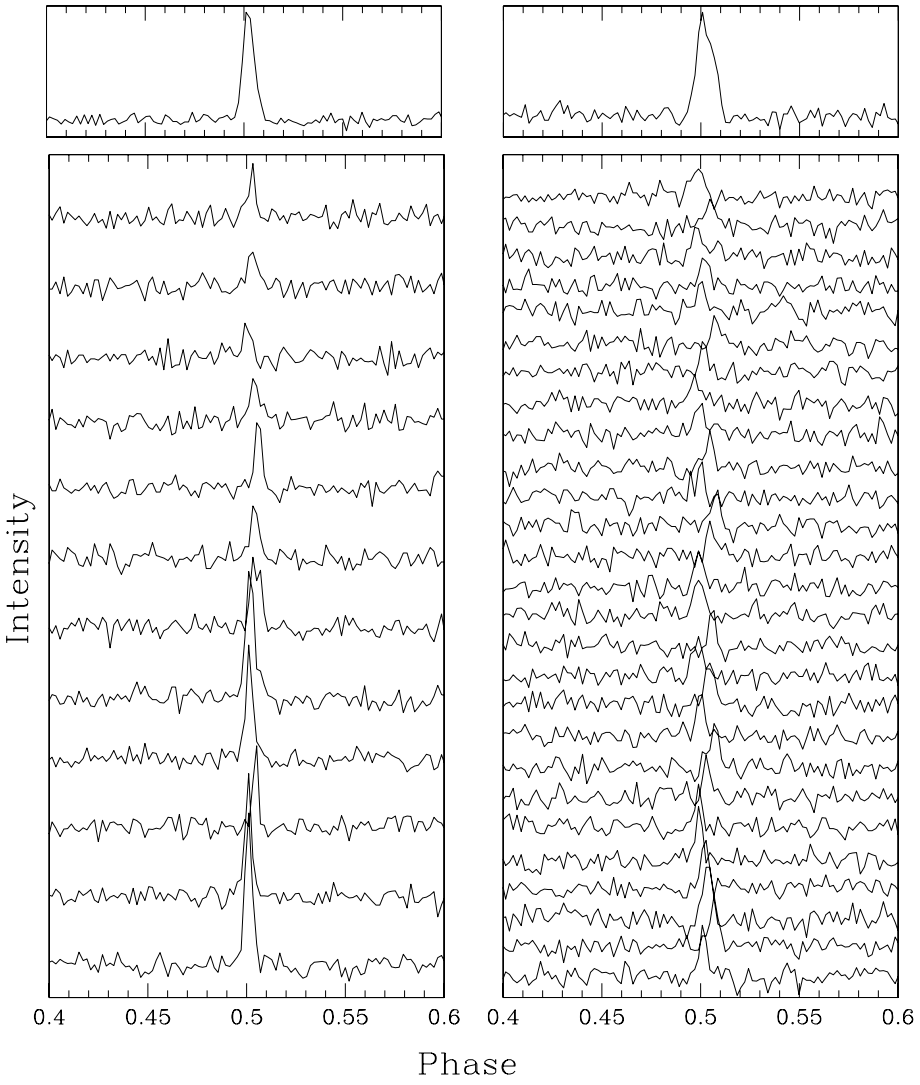

Figure 2. All of the single pulses detected in a single 1.4-GHz Parkes observation of (left) J1317−5759 (MJD 53490) and (right) J1913+1330 (MJD 53156), along with the composite profiles (top) made of all detected single pulses from each observation. The observations were 1- and 2-h long, and there are 12 and 27 single pulses for J1317−5759 and J1913+1330, respectively. Note that none of these pulses is consecutive, and the spacing between the pulses varies.

Table 2. Periods, period derivatives, MJDs of the epoch used for the period determination, the average pulse widths at 50 per cent of the peak, the rms values of the post-fit timing residual, numbers of pulses included in the timing solution, the MJD ranges covered, the numbers of epochs and the rates of pulse detection. The numbers in parentheses after P and $\dot{P}$ the 1σ errors reported by TEMPO. The numbers in parentheses after w_{50} are the standard deviations. The numbers in parentheses after the total number of observed epochs are the number of epochs with at least one pulse detected. For J1913+1330, the first/second numbers are for the Parkes/Lovell telescopes. The rate of pulse detection is much lower for the Lovell telescope due to the smaller bandwidth and worse environment for RFI.

Name	P (s)	$\dot{P}$ (10^{-15})	Epoch (MJD)	w_{50} (ms)	Residual (ms)	$N_{\rm p}$	Data span (MJD)	$N_{\rm e}$	Rate (h^{-1})
J0847−4316	5.9774927370(7)	119.94(2)	53816	27(13)	11.2	138	52914–54716	61(34)	2.1
J1317−5759	2.64219851320(5)	12.560(3)	53911	12(5)	5.0	249	53104–54717	69(60)	5.2
J1444−6026	4.7585755679(2)	18.542(8)	53893	21(7)	3.2	42	53104–54682	71(25)	0.85
J1826−1419	0.770620171033(7)	8.7841(2)	54053	2(1.1)	0.8	46	53195–54909	57(18)	1.0
J1846−0257	4.4767225398(1)	160.587(3)	53039	15(6)	5.4	42	51298–54780	49(21)	1.2
J1913+1330	0.92339055858(2)	8.6799(2)	53987	2(0.7)	1.1	189(159)	53035–54938	26(17), 62(24)	13, 1.5

frequency second derivative of $4.6(1) \times 10^{-25}\,{\rm s}^{-3}$ was necessary to fit the data because of a large amount of timing noise. Note that our period derivative measurement for J1846−0247 is consistent with the upper limit presented in Archibald et al. (2008). There is no evidence for any binary companions to these objects. We see no evidence for glitches, as seen for J1819–1458 (Lyne et al. 2009). To ensure that the quoted errors in our final model parameters are robust, we multiply our formal TOA uncertainties by the factor

necessary for the reduced chi-squared of our residuals to be equal to one.

In Table 1, we list the offsets of the timing-derived positions from the discovery positions for the RRATs. For two of the RRATs, the timing-derived position actually lies outside of the 14-arcmin-diameter discovery beam of the only PMPS detection. Because of the sporadic nature of the emission from these sources, they were not discovered in the PMPS pointings that were closer to their actual positions. This illustrates the caution with which one must take the discovery positions for these extreme objects.

For RRATs with detections at multiple centre frequencies, the DMs in Table 1 were obtained by fitting TOAs at multiple frequencies. For RRATs with detections only at 1.4 GHz, DMs were calculated by fitting TOAs in four subbands of the 1.4-GHz bandpass. The extremely accurate DM for J1913+1330 results from including the sensitive low-frequency observations with the Arecibo telescope in our timing solution. The Arecibo TOAs have formal uncertainties a factor of ∼3 smaller than the Parkes TOAs. However, despite this increased sensitivity, the source was only detected at one of five epochs with Arecibo due to the short observation time. We therefore do not list the overall pulse statistics for the Arecibo observations.

The post-fit timing residuals for all six RRATs are presented in Fig. 3. The average rms residual ranges from 0.8 ms (for J1826−1419) to 11.2 ms (for J0847−4316), or roughly 1–2 per cent of the pulse period. These are roughly equal to the widths of the composite pulses for these objects, listed in Table 2. For the six RRATs discussed in this paper, we see no evidence for the 'banding' structure seen in the J1819−1358 residuals (Esamdin et al. 2008; Lyne et al. 2009), and the composite profiles of these RRATs appear to be single. The pronounced non-uniformity in the residual spacing for J1913+1330 in Fig. 3 is due primarily to gaps in observing coverage. For the other RRATs, any non-uniformity is likely to arise from intrinsic variability in the rate of pulse emission. This time variability of burst rates will be discussed in more detail in a follow-up paper.

4 DISCUSSION

Keane & Kramer (2008) found that the Galactic supernova rate was insufficient to account for the entire population of neutron stars, including radio pulsars, INSs, magnetars and the central compact objects. Evolution among the various types of neutron stars could go a long way towards solving this problem. It is therefore important to compare the spin-down properties of the RRATs with those of these other objects. In Table 3, for all of the six objects, we list the inferred surface dipole magnetic field, the characteristic age, the spin-down energy-loss rate and the magnetic field strength at the light cylinder. In Fig. 4, we place the RRATs on a P–$\dot{P}$ diagram

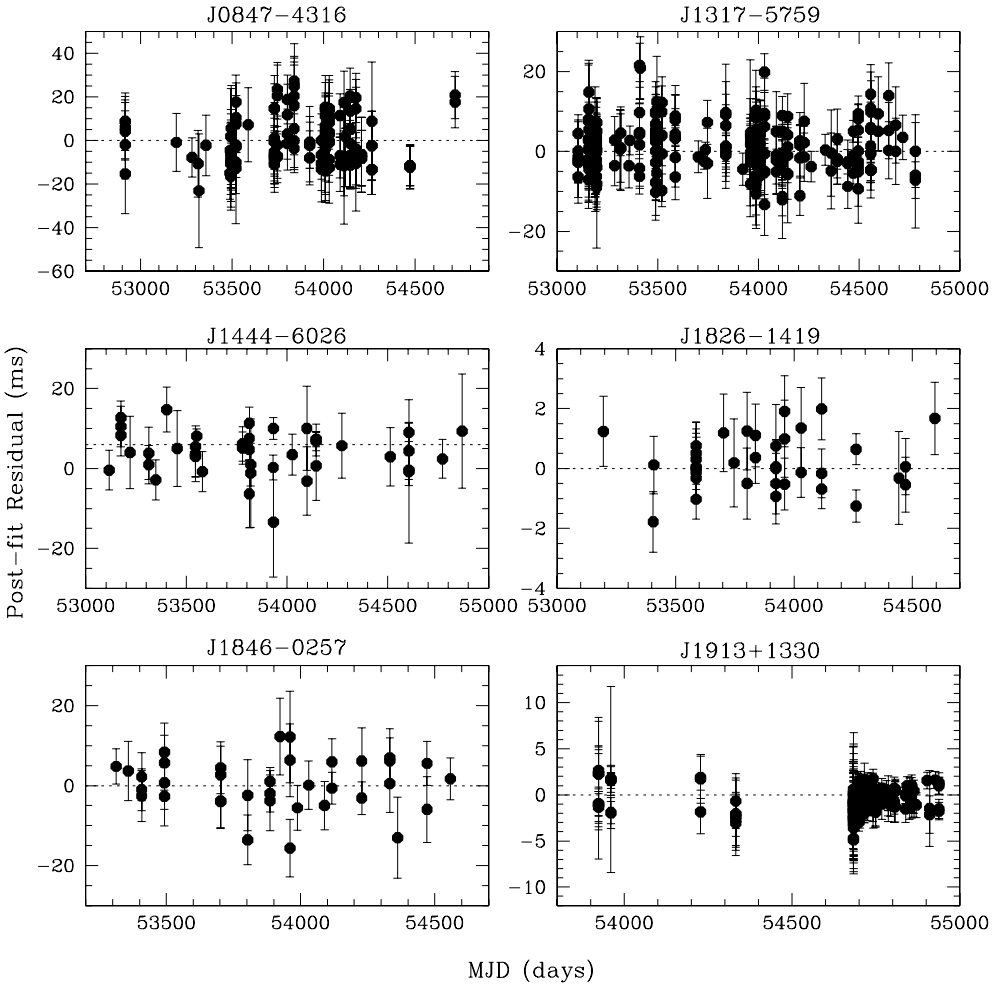

Figure 3. Post-fit timing residuals for all six RRATs. The error bars show 1σ errors on the individual TOAs. All data (i.e. from all frequencies and telescopes) have been included.

Table 3. Base 10 logarithms of the derived parameters characteristic age, surface dipole magnetic field strength, rotational energy-loss rate and magnetic field strength at the light cylinder. See Lorimer & Kramer (2005) for definitions of these parameters.

Name	log [τ_c] (yr)	log [B] (G)	log[$\dot{E}$] (erg s^{-1})	log [B_{LC}] (G)
J0847−4316	5.9	13.4	31.3	0.1
J1317−5759	6.5	12.8	31.4	0.5
J1444−6026	6.6	13.0	30.8	−0.1
J1826−1419	6.1	12.4	32.9	1.7
J1846−0257	5.6	13.4	31.8	0.4
J1913+1330	6.2	12.4	32.6	1.5

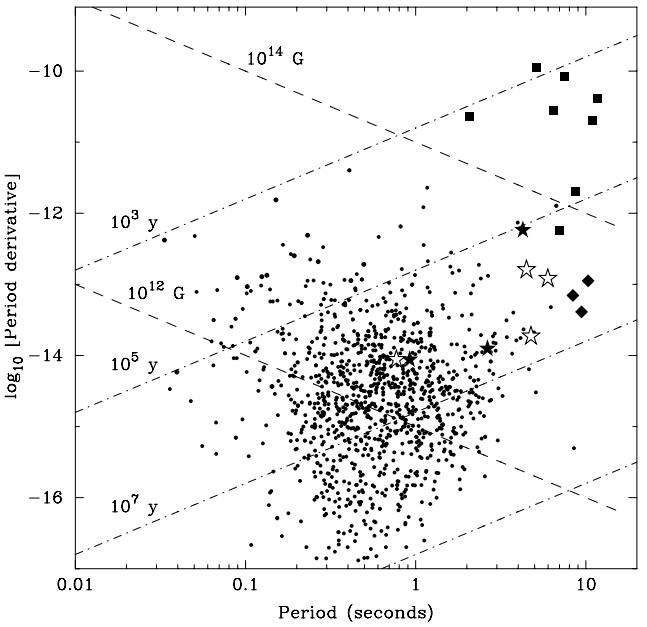

Figure 4. P versus $\dot{P}$ for pulsars (dots; Manchester et al. 2005), magnetars (squares; Camilo et al. 2007), the original three RRATs with measured periods and period derivatives (red stars; McLaughlin et al. 2006) and the three INSs with measured period and period derivative (diamonds; Kaplan & van Kerkwijk 2009). The RRATs with new timing solutions presented in this paper are marked by green stars. Constant characteristic age and constant inferred surface dipole magnetic field strength are indicated by dashed lines.

with other populations of neutron stars. The spin-down properties of J1826−1419 and J1913+1330 are remarkably similar to each other and place them solidly within the normal radio pulsar population. This would support models which suggest that the RRATs are simply normal pulsars at the tail end of the (largely unexplored) intermittency distribution (Weltevrede et al. 2006), which attribute the RRATs' unusual emission to external factors (e.g. Li 2006; Cordes & Shannon 2008) or which theorize that the emission is similar to that of normal nulling pulsars (e.g. Zhang et al. 2007). Two other RRATs, J1317−5759 and J1444−6026, have long spin periods and large characteristic ages and are nearing the 'death line' for radio pulsars (Chen & Ruderman 1993). These properties suggest that these RRATs are older pulsars whose radio emission is slowly turning off (e.g. Zhang et al. 2007). Two other RRATs for which we have recently obtained solutions, J0847−4316 and J1846−0257, have high magnetic fields and are in a region of P–$\dot{P}$ space devoid of radio pulsars. The proximity of these objects to the X-ray detected but radio-quiet INS suggests that these sources may be transition objects between normal radio pulsars and INSs, an idea supported by the population analysis of Keane & Kramer (2008). It should be noted that INS may not be an intrinsically radio-quiet population. Kondratiev et al. (2009) show that the radio non-detections of INS can easily be attributed to beaming effects. The remaining RRAT, J1819−1458, for which a detailed analysis is reported in Lyne et al. (2009), has a high magnetic field and spin-down parameters similar to both some high magnetic field radio pulsars and magnetars.

To test whether the distributions of the derived parameters of the RRATs are consistent with those of the normal pulsar population, we performed a Kolmogorov–Smirnoff (KS; see e.g. Press et al. 1986) test on the distributions of RRATs and all of the pulsars detected in the PMPS (see Fig. 5). We use the more uniform PMPS sample, as opposed to all radio pulsars, to mitigate selection effects. For the RRATs distribution, we include all PMPS-detected RRATs (McLaughlin et al. 2006; Keane et al. 2009). In Table 4, we list $\mathcal{P}_{KS}$, or the probability that the two distributions are drawn from the same parent distribution. We also list $\mathcal{P}_{ran}$, or the probability of getting a $\mathcal{P}_{KS}$ as low or lower, as determined by simulations of 100 000 trials where we randomly select values from the PMPS sample.

For the period distribution, we include all PMPS-detected RRATs with measured periods. This includes 10 RRATs from McLaughlin et al. (2006) and eight (all but J1841−14) from Keane et al. (2009). While for the derived parameters we include the six RRATs discussed in this paper and J1819−1458. The probabilities that the periods and magnetic fields of the RRATs and normal pulsars are drawn from the same parent distributions are small ($< 10^{-3}$), with the RRATs having longer periods and higher magnetic fields. This suggests that long-period neutron stars with higher magnetic fields are more likely to manifest themselves as RRATs than are shorter period or lower magnetic field neutron stars.

We believe that the effect is real and not due to a bias against short-period objects. Following McLaughlin & Cordes (2003), we can show that a single-pulse search will be superior to a periodicity search for periods between $T_{obs}g^2/4 < P < T_{obs}g$, where T_{obs} is the observation length and g is the fraction of neutron star rotations where a pulse is emitted. For $g = 0.001$ and $T\text{-}1_{obs} = 35$ min (i.e. the length of the PMPS observations), this period range is 0.5 ms to 126 s. Therefore, for a pulse emission rate as high as one per 1000 pulses (i.e. similar to J1913+1330), the single-pulse search will result in higher signal-to-noise ratios than a periodicity search for any reasonable periods. For lower pulse emission rates of $g = 10^{-4}$ (i.e. similar to J1826−1419), the single-pulse search will result in higher signal-to-noise ratios than periodicity search for an even broader range of periods. It is only when we approach much higher pulse emission rates (i.e. g close to 0.01) that selection effects against short-period objects become important. We therefore believe that shorter period objects with similar rates of pulse emission to these six sources would also have appeared as RRATs in the PMPS. As there is no bias against period derivative in this survey, we infer that the relationship between RRAT behaviour and both period and magnetic field is robust. The characteristic age, energy-loss rate and magnetic field at the light cylinder distributions of normal pulsars and RRATs are consistent. This suggests that the RRATs emission behaviour is not determined solely by any of these quantities. In Table 1, we list distances inferred from the best-fitting DMs using the Cordes & Lazio (2002) model for Galactic electron density. We found that the probability that the PMPS-detected RRATs distribution [including 11 RRATs from McLaughlin et al. (2006) and 10 RRATs from Keane et al. (2009)] and the PMPS distribution are drawn from the same parent distribution is 4×10^{-2}, with the RRAT population being slightly more nearby. However, due to the

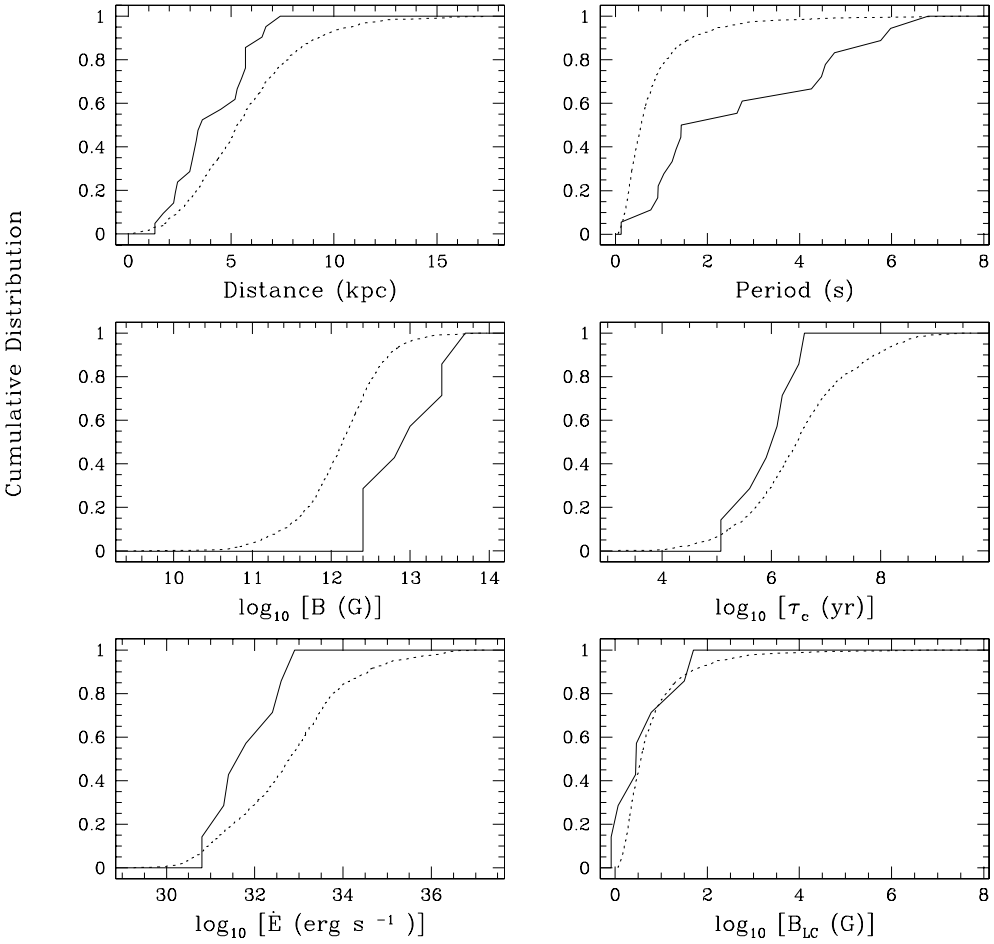

Figure 5. Cumulative probability distributions for distance, period, magnetic field, characteristic age, spin-down energy-loss rate and magnetic field at the light cylinder for RRATs (solid lines) and all PMPS-detected non-recycled pulsars (dashed lines). The RRAT sample includes all PMPS-detected RRATs [10 from McLaughlin et al. (2006) and eight (all but J1841−14, which can be detected through its time-averaged emission) from Keane et al. (2009) for P, 11 from McLaughlin et al. (2006) and 10 (again excluding J1841−14) from Keane et al. (2009) for d and six from this paper and one from Lyne et al. (2009) for the other parameters]. The PMPS sample includes 1004 (for P and d) and 984 (for other parameters) pulsars. Note that while the difference between the two CDFs seems smaller for d than for some other parameters, there are more measured distances and therefore this difference is more significant.

Table 4. Measured or derived parameter, the probability that the RRATs and all PMPS-detected pulsars are drawn from the same parent distribution and the probability of measuring a $\mathcal{P}_{\rm KS}$ as low or lower in our simulations.

Parameter	$\mathcal{P}_{\rm KS}$	$\mathcal{P}_{\rm ran}$
d	4×10^{-2}	4×10^{-2}
P	7×10^{-7}	$< 1 \times 10^{-7}$
B	8×10^{-4}	4×10^{-4}
$\tau_{\rm c}$	0.3	0.3
$\dot{E}$	0.1	0.1
$B_{\rm LC}$	0.5	0.5

significant selection effects involved in distance distributions it is difficult to draw conclusions from this weak correlation.

Pulsars which emit giant pulses have been shown (e.g. Knight et al. 2005) to have values of magnetic field at the light cylinder $B_{\rm LC}$ greater than 10^5 G and spin-down rotational energy loss $\dot{E}$ values greater than 10^{35} erg s^{-1}. The values of $B_{\rm LC}$ and $\dot{E}$ for all of the RRATs are many orders of magnitude below these values, suggesting that the RRAT's emission mechanism is very different. The pulses of the RRATs are also wider than the widths of pulsar giant pulses, which have widths of much less than 1 ms (e.g. Bhat, Tingay & Knight 2008). They range from 2 to 30 ms, with duty cycles ranging from 0.21 per cent (for J1913+1333) to 0.45 per cent (for J0847−4316 and J1317−5759).

5 CONCLUSIONS AND FUTURE WORK

We have presented a method for timing pulsars through their individual pulses, and have applied this method to RRAT sources originally discovered in the PMPS. Our work results in four new timing solutions, resulting in seven of 11 of these RRATs having phase-connected solutions. We find that the period and magnetic field distributions of RRATs and normal pulsars are different, and that this difference cannot be explained by selection effects. This suggests that the unusual emission behaviour of the RRATs may be related to their long periods and high magnetic fields. More phase-connected solutions are necessary to determine any evolutionary relationships between these objects and the long-period, high-magnetic-field populations of magnetars and X-ray-detected INSs. The high-energy observations enabled by the new timing

positions presented in this paper will be crucial for testing these relationships.

There remain four RRATs from the original PMPS analysis for which we do not yet have phase-connected solutions. One of these, J1839−01, has only been detected once despite multiple attempts. The remaining three RRATs have pulses that are too sporadic and weak to be timed with the Parkes telescope and are the subjects of intense low-frequency Green Bank Telescope and Arecibo observing campaigns. These campaigns, and the properties of the RRATs discussed in this paper at low frequencies, will be the subject of a follow-up paper.

ACKNOWLEDGMENTS

We thank all on the Parkes Multibeam Survey team for assistance with the Parkes radio observations. We are grateful to Aris Karastergiou for useful comments on the manuscript. MAM, JJM and DRL are supported by a WV EPSCoR grant. EFK acknowledges the support of a Marie-Curie EST Fellowship with the FP6 Network 'ESTRELA' under contract number MEST-CT-2005-19669.

REFERENCES

Archibald A. M., Kaspi V. M., Livingstone M. A., McLaughlin M. A., 2008, ApJ, 688, 550
Becker W., Trümper J., 1997, A&A, 326, 682
Bhat N. D. R., Tingay S. J., Knight H. S., 2008, ApJ, 676, 1200
Camilo F., Ransom S. M., Halpern J. P., Reynolds J., Helfand D. J., Zimmerman N., Sarkissian J., 2006, Nat, 442, 892
Camilo F., Ransom S. M., Halpern J. P., Reynolds J., 2007, ApJ, 666, L93
Champion D. J. et al., 2005, MNRAS, 363, 929
Chen K., Ruderman M., 1993, ApJ, 408, 179
Cordes J. M., Lazio T. J. W., 2002, preprint (astro-ph/0207156)
Cordes J. M., Shannon R. M., 2008, ApJ, 682, 1152
De Luca A., Caraveo P. A., Mereghetti S., Negroni M., Bignami G. F., 2005, ApJ, 623, 1051
Deneva J. S., Cordes J. M., McLaughlin M. A., 2009, ApJ, 703, 2259
Esamdin A., Zhao C. S., Yan Y., Wang N., Nizamidin H., Liu Z. Y., 2008, MNRAS, 389, 1399
Haslam C. G. T., Klein U., Salter C. J., Stoffel H., Wilson W. E., Cleary M. N., Cooke D. J., Thomasson P., 1981, A&A, 100, 209
Hessels J. W. T., Ransom S. M., Kaspi V. M., Roberts M. S. E., Champion D. J., Stappers B. W., 2008, in Bassa C., Wang Z., Cumming A., Kaspi V. M., eds, AIP Conf. Ser. Vol. 983, 40 Years of Pulsars: Millisecond Pulsars, Magnetars and More. Am. Inst. Phys., New York, p. 613
Kaplan D. L., 2008, in Yuan Y.-F., Li X.-D., Lai D., eds, AIP Conf. Ser. Vol. 968, Astrophysics of Compact Objects. Am. Inst. Phys., New York, p. 129
Kaplan D. L., van Kerkwijk M. H., 2009, ApJ, 692, L62
Karastergiou A., Hotan A. W., van Straten W., McLaughlin M. A., Ord S. M., 2009, MNRAS, 396, L95
Keane E. F., Kramer M., 2008, MNRAS, 391, 2009
Keane E., Ludovici D. A., Kramer M., Lyne A. G., McLaughlin M. A., Stappers B. W., 2009, MNRAS, in press (arXiv:0909.1924)
Keith M. J., Eatough R. P., Lyne A. G., Kramer M., Possenti A., Camilo F., Manchester R. N., 2009, MNRAS, 395, 837
Knight H. S., Bailes M., Manchester R. N., Ord S. M., 2005, ApJ, 625, 951
Knight H. S., Bailes M., Manchester R. N., Ord S. M., Jacoby B. A., 2006, ApJ, 640, 941
Kondratiev V. I., McLaughlin M. A., Lorimer D. R., Burgay M., Possenti A., Turolla R., Popov S. B., Zane S., 2009, ApJ, 702, 692
Lawson K. D., Mayer C. J., Osborne J. L., Parkinson M. L., 1987, MNRAS, 225, 307
Li X.-D., 2006, ApJ, 646, L139
Lorimer D. R., Kramer M., 2005, Handbook of Pulsar Astronomy. Cambridge Univ. Press, Cambridge
Luo Q., Melrose D., 2007, MNRAS, 378, 1481
Lyne A. G., McLaughlin M. A., Keane E., Kramer M., Espinoza C. M., Stappers B. W., Palliyaguru N. T., Miller J., 2009, MNRAS, this issue (doi:10.1111/j.1365-2966.2009.15668.x)
McLaughlin M. A., Cordes J. M., 2003, ApJ, 596, 982
McLaughlin M. A. et al., 2006, Nat, 439, 817
McLaughlin M. A. et al., 2007, ApJ, 670, 1307
Manchester R. N. et al., 2001, MNRAS, 328, 17
Manchester R. N., Hobbs G. B., Teoh A., Hobbs M., 2005, AJ, 129, 1993
Popov S. B., Turolla R., Possenti A., 2006, MNRAS, 369, L23
Press W. H., Flannery B. P., Teukolsky S. A., Vetterling W. T., 1986, Numerical Recipes: The Art of Scientific Computing. Cambridge Univ. Press, Cambridge
Rea N. et al., 2009, ApJ, 703, L41
Redman S. L., Rankin J. M., 2009, MNRAS, 395, 1529
Weltevrede P., Stappers B. W., Rankin J. M., Wright G. A. E., 2006, ApJ, 645, L149
Woods P. M., Thompson C., 2006, in Lewin W., van der Klis M., eds, Compact Stellar X-ray Sources, Cambridge Astrophys. Ser. No. 39. Cambridge Univ. Press, Cambridge, p. 547
Zhang B., Gil J., Dyks J., 2007, MNRAS, 374, 1103

This paper has been typeset from a TEX/LATEX file prepared by the author.